

# CVD diamond-based semi-transparent beam-position monitors for synchrotron beamlines: preliminary studies and device developments at CEA/Saclay

P. Bergonzo,\* D. Tromson and C. Mer

LIST (CEA - Recherche Technologique)/DETECS/SSTM, CEA/Saclay, France.

E-mail: philippe.bergonzo@cea.fr

Polycrystalline diamond synthesized using the chemical vapour deposition (CVD) technique can be used to fabricate new types of photodetectors for the characterization of X-ray light in synchrotron beamlines. Since diamond exhibits a low absorption to low-energy photons, such devices allow beam-position monitoring with very little beam attenuation at photon energies as low as 2 keV up to 15–20 keV. Here it is shown how diamond-based devices can simply be processed as ionization chambers for advanced semi-transparent position monitoring with high position resolution ( $<2\ \mu\text{m}$ ). Other configurations using the same principle can also enable in-line field profiling. It is also shown what can be expected from these devices in terms of performances, signal-to-noise ratios and reliability, together with their inherent limitations caused by the presence of defects in polycrystalline materials. In particular, diamond devices with extremely low carrier lifetimes, owing to quenched transport properties, could also be of particular interest for the characterization of the temporal structure of synchrotron light. Interest in these devices lies in the permanent insertion into beamlines and withstanding high levels of radiation for continuous beam monitoring.

**Keywords:** CVD diamond; BPM; detectors.

## 1. Introduction

Radiation detectors based on the photoconductive properties of chemical-vapour-deposited diamond have been studied since the early 1970s (Kozlov *et al.*, 1974). This proved how remarkable the material could be, but also demonstrated that extremely few natural stones could exhibit the required photoconduction properties, particularly in terms of reliability, stability and uniformity. More recent studies have focused on the ability to grow high-quality synthetic diamonds that could be used as solid-state ionization-chamber radiation detectors for several families of applications, dedicated to specific needs where no other materials could withstand the ambient conditions (*e.g.* corrosive or highly ionizing environments) (Bergonzo, Foulon *et al.*, 2000; Mer *et al.*, 2004) where the diamond properties fit with the application requirements (*e.g.* speed, low atomic number, tissue equivalence *etc.*) (Foulon *et al.*, 1998; Guerrero *et al.*, 2004).

In fact, diamond exhibits several remarkable properties in comparison with other semiconducting materials (Franklin *et al.*, 1992), such as high band gap, high electron–hole pair mobility, short carrier lifetime and extreme resilience to harsh environments. The recent progress in diamond growing tech-

niques has made the synthesis of this material readily available. Synthetic diamond layers can be grown using the microwave-enhanced chemical vapour deposition (CVD) technique from the dissociation of a methane and hydrogen precursor mixture. A polycrystalline material can be obtained on large-area substrates such as silicon. After a first step of nucleation, columnar growth of diamond occurs resulting in non-homogeneous grain size in the material volume, with the biggest grain size on the front layer of about 10% of the grown layer thickness. Under optimized conditions, electronic-grade polycrystalline diamond is achievable. However, on diamond itself, homoepitaxial growth can lead to the formation of monocrystalline layers, and under particular conditions (Scarsbrook *et al.*, 2001) extreme purity materials with exceptional performances have been grown (Isberg *et al.*, 2002). However, such layers are limited to the size of the substrates on which they have been grown, and therefore areas above 5 mm in diameter can rapidly become extremely challenging to make.

This article focuses on the possibilities of using polycrystalline synthetic diamond for beam metrology on synchrotron beamlines. Advances in experiments using synchrotron light sources have generated a demand for

permanent in-line radiation-hard X-ray monitors in the energy range 1.5 keV to 25 keV. For example, for demanding experiments such as XAFS on ultra-dilute samples or polarization-dependent X-ray spectroscopy it may become necessary to control the beam instabilities with respect to both position and time. Also, in the field of protein crystallography, high-throughput purification and crystallization methods are capable of producing very high quality but very small protein crystals which decay rapidly in strong undulator beams. In addition, beamlines have to focus to smaller beam spots and are thus subject to systematic errors caused by relative beam movements. In these respects there is a great need to be able to trace beam fluctuations or vibrations. It is of interest to install multiple beam-position monitors into a beamline, and to do this without seriously impairing the quality or intensity of the beam available to the end experiment. The ideal device thus consists of a high-precision high-bandwidth invisible beam monitor with high dynamic range owing to different beam modes and decaying synchrotron currents.

It thus becomes evident that CVD diamond exhibits two distinct advantages over all other detector materials for these types of requirements: its high radiation hardness allowing long-term *in situ* analysis, and its low atomic number resulting in a low X-ray absorption cross section. This combination enables thin-film photodetectors to be inserted permanently in synchrotron beamlines causing little intensity perturbations downstream. Also, the ability to reach fast repetition rates has been demonstrated, up to the frequencies used on synchrotron beamlines, and this could be of high benefit where fast response times are needed.

### 2. State of the art

An accurate knowledge of the position of the X-ray beam with a good time resolution is becoming a critical requirement for many synchrotron beamlines. It is of interest to install several beam-position monitors into a beamline without seriously impairing the quality or intensity of the beam available to the end experiment. Among the existing competing technologies that could be used for synchrotron beam metrology, diamond has to prove that it surpasses other techniques such as those based on gas ionization chambers, metallic blades or using other semiconductor detectors. In fact, several techniques have proven promising at various synchrotron sources, and are described by Schulze-Briese *et al.* (2001), Alkire *et al.* (2000), van Silfhout (1999), Loudin *et al.* (1998), Holldack *et al.* (2001) and Aoyagi *et al.* (2001). For example, quadrant detectors of the type developed by Alkire *et al.* (2000) are capable of high precision but at present are not used in white-beam applications. Other approaches specifically relying on diamond have also demonstrated high potential as possible beam-position monitors, such as blades (Kuzay & Shu, 1995) and ionization chambers (Sakae *et al.*, 1997; Shu, 1999; Shu & Kuzay, 1995). These techniques have proven to be well adapted to the specific properties of the light conditions (intensity, energy, fluence) for which they have been developed. For our particular case where we wish to develop a device that can be

permanently inserted into beamlines with little attenuation, the greatest competitor to diamond remains silicon. In fact, in beamline metrology the conditions are often a lot less hostile than in front-ends, and therefore do not necessitate the use of such a radiation-hard material as diamond. For example, recent devices have been tested based on ultra-thin silicon membranes based on SOI (silicon-on-insulator) technology that prove to be extremely stable and reliable. The drawback with silicon is the higher attenuation owing to its higher *Z*, and also the fact that using relatively high-*Z* single crystals results in glitches, *i.e.* the sudden change of apparent energy transmission owing to the diffraction of the beam by the crystal. This can be a problem for applications where the energy is tuned, and namely for all spectroscopy experiments (XAFS, QEXAFS, XANES *etc.*). These glitches in the transmission are well known by beamline users and can pollute experiments up to the point where such devices become forbidden.

Other techniques may also be based on diamond layers, even though they do not rely on the direct measurement of the photo-induced currents in the material. Of these, devices based on the X-ray-induced photoemission from diamond surfaces can be of interest. Provisional measurements have been conducted at LURE (Laboratoire pour l'Utilisation du Rayonnement Electromagnétique, Orsay, France) (Ascarelli *et al.*, 2001) and a beam-position monitoring system based on photoemission was developed at the SIBERIA synchrotron and tested elsewhere (Loudin *et al.*, 1998). The possibility of using diamond as the photoemissive source can be of interest, especially knowing that surface emission properties can be strongly enhanced by surface treatments such as exposure to hydrogen plasmas (Ristein *et al.*, 2001). Such tests have been conducted recently at ESRF (European Synchrotron Radiation Facility) but did not seem to be as convincing because the surface emission properties were strongly altered in the vacuum (Barrett *et al.*, 2002).

Several groups have also thought of using diamond as a fluorescent screen, since synthetic diamond has proven to luminesce under X-ray light (Nam *et al.*, 1992). However, here the resolution in terms of beam-position monitoring relies on the precision of the remote camera that is probing the position of interaction on the diamond layer, and generally does not allow very high precision. Few measurements have already been begun on ESRF beamlines in conjunction with beamline scientists for evaluation of the perspectives of this technique (J.-A. Nielsen, private communication). The main drawback of this approach is the relatively poor precision for beam-position measurements. The technique could also be of interest for intensity measurements, but non-linearities as a function of the X-ray fluency have been observed. These are caused by the fact that the X-ray photoluminescence relies on the presence of defects in the synthetic diamond, and that their irradiation, and thus local heat at high fluency, modifies trapping level density populations and thus causes non-linearities, especially under intense photon fluences (G. Naylor, private communication).

Finally, a further approach with diamond detectors is to investigate the possibilities of artificial diamond single crystals.

This approach is currently being evaluated in a separate project between Element Six (DeBeers) and ESRF, where recent investigations were conducted (Morse *et al.*, 2006). Indeed, the possibility of using diamond single crystals is tempting, even though the difficulty of reaching large single-crystal surface areas (>5 mm diameter) is known and that the processing costs may be significant in order to prepare the diamond single-crystal surfaces for device fabrication. Nevertheless, it is clear that the difficulties encountered using single-crystal ultra-thin silicon devices such as glitches will also be the concern of such single-crystal diamond devices, and must be evaluated further.

From these approaches our goal has been to investigate the possibility of directly using highly transparent diamond thin membranes, that are polycrystalline and for which fabrication does not require complicated processing steps. These are used as photoconductors permanently inserted in beamlines, the main topic discussed in this article.

### 3. Evaluation of the ideal performance of diamond ionization-chamber detectors

As discussed above, the main domain of interest starts around 4 keV, the energy at which a 20 μm diamond layer still transmits 80%. In the higher energy domain, the material rapidly becomes less interesting since very high thicknesses become necessary, and furthermore the competition with silicon becomes greater. In practice we can state that an upper limit of 17–20 keV constitutes a higher limit. The theoretical expression of the current produced by a constant charge generation for a constant electric field and ohmic contacts is

$$I = q(E_{\text{dep}}/\epsilon_p)(\mu\tau E/L), \quad (1)$$

where  $q$  is the electronic charge,  $E_{\text{dep}}$  (keV s<sup>-1</sup>) is the deposited energy per unit of time,  $\epsilon_p$  is the mean energy to create an electron–hole pair (~13 eV),  $\mu$  and  $\tau$  are the carrier mobility and lifetime,  $E$  is the electric field and  $L$  is the distance between the two electrodes (Kozlov *et al.*, 1975). The ratio  $\mu\tau E/L$  defines the device efficiency, in the current mode, which can be defined as the ratio between the induced current and the deposited energy per unit of time. Values may vary from 20% on poor quality materials up to 100% on the best materials, assuming no persistent photocurrent nor space-charge-driven photocurrents. This will be discussed in more detail in §4. In fact, poor device efficiency relates to charge losses and is common in polycrystalline CVD diamond and assumed to be caused by grain boundaries or by defects, resulting in the shortening of the generated charge drift distance (Souw & Meilunas, 1997).

Assuming a device efficiency of unity, equation (1) enables us to evaluate the absolute photocurrents that could be expected using this type of device. In fact, if we consider that the ideal device should transmit between 80% and 95% of the incoming incident energy, it is clear that optimizing the transmission and the device signal requires adapting the thickness of the diamond detector to the incident photon

energy. If the device is too thin, then the photocurrent may be too weak to be measurable and lead to poor signal-to-noise and thus altered performances, whereas too thick a device would be too absorbing. This is plotted ideally in Fig. 1 assuming a 10<sup>10</sup> photon s<sup>-1</sup> fluency, and knowing that the theoretical signal is directly proportional to the photon fluency. We can see the importance of optimizing the thickness to the incident photon energy, as well as from the expected current values which have to be measured.

### 4. Defects

Severe detrimental effects occur from the presence of diamond and significantly alter the detection properties of devices. In fact, it is clear that the response of diamond ionization chambers is reduced because of defects and impurities. If their state is modified either because of the ionization mechanism (trapping) or because of a significant elevation in temperature (trapped carrier release), the internal electric field in the device as well as the carrier lifetime can be modified, thus altering the response of the detector (Souw & Meilunas, 1997). This capture/release mechanism of carriers on trapping levels induces a space-charge build-up that has been clearly evidenced by thermally stimulated measurements (Tromson *et al.*, 2000). According to the technique used to calculate the energy levels that are released at around 573 K, values close to 1.2 eV are probed. Similar levels are commonly observed in natural diamonds and have been attributed to nitrogen impurities. The filling of these deep traps prior to measurements leads to improved transport properties. This can be achieved by irradiating the material under a 50 kV X-ray tube at a typical dose of 10 Gy. This procedure, called the ‘priming’ or ‘pumping’ phenomenon, is known to improve the collection efficiency dramatically (Behnken *et al.*, 1998). Thus it is a common observation that the progressive irra-

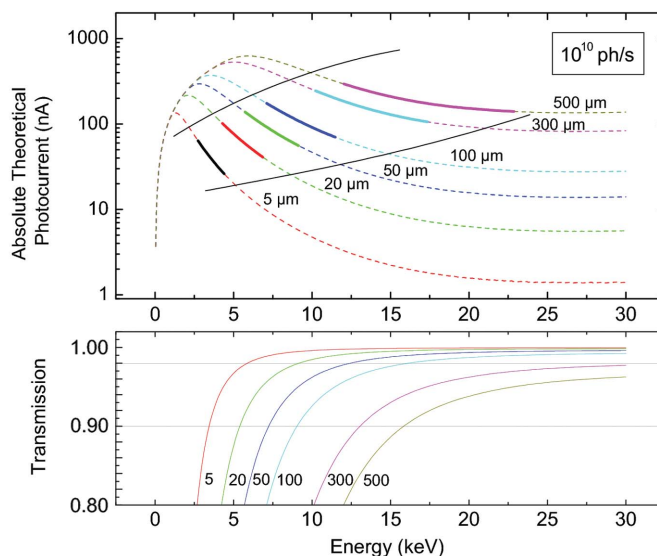


**Figure 1** Theoretical photocurrents in semi-transparent diamond ionization-chamber devices for beam monitoring. Expected values are given for 10<sup>10</sup> photons s<sup>-1</sup>, but remain directly proportional to the photon fluency.

diation of CVD diamond ionization chambers causes an increase in the detector sensitivity. In the case of X-ray irradiation in a synchrotron, the dose can be estimated from the knowledge of the photon fluency and energy: typically, if we consider even a low  $10^{10}$  photons  $s^{-1}$  at 9 keV impinging on a diamond sample of thickness 100  $\mu m$  over a 50  $\mu m$  diameter spot, we obtain a corresponding dose of the order of 2 kGy. Comparing this value with the 10 Gy typical dose necessary to prime a diamond device, the present estimation shows that diamond is immediately self-primed even under conditions where the fluency is low. This implies that the trapping/detrapping instabilities will not be apparent and should have no negative effect upon the use of diamond for synchrotron beam metrology applications.

One other detrimental consequence of the presence of electrical defects is the effect of polarization: if the impinging radiation tends to alter the trapping level status non-homogeneously throughout the device volume, modification of the electric field distribution may result, leading to inhomogeneous and unstable photocurrents. These effects relative to the radiation-induced polarization are predominant in thick layers when used for short-range particle detection. In the case of synchrotron X-rays, since we want to induce almost no attenuation to the incoming X-ray beam, the diamond thickness is kept very low compared with the penetration depth of the photons, and this effect is again negligible.

The presence of traps may also affect the decay time of the detector after a pulsed excitation. Fig. 2 shows the responses of two devices under X-ray pulsed excitation generated by a synchrotron light source (at LURE). The pulse duration is estimated at 600 ps FWHM with a period of 120 ns that is expected to be long with respect to the signal decay time in diamond. The curve reveals the extreme differing qualities of the CVD diamonds probed, as the signal in the lower figure exhibits fast decay characteristics, whereas the response shown

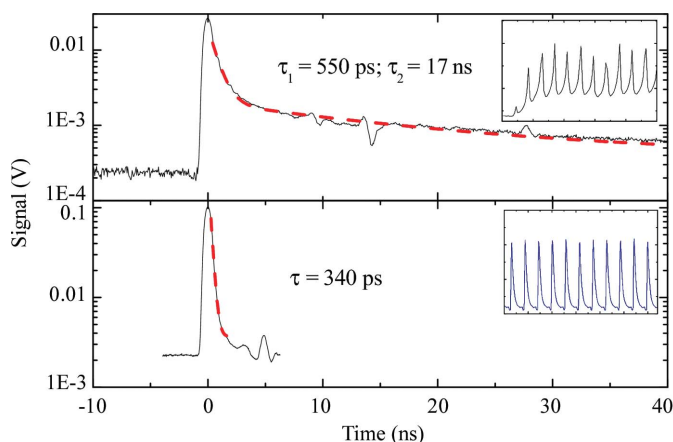


**Figure 2** Response obtained on two CVD diamond devices (same contact geometries and electric fields) to 1 keV X-ray pulses (FWHM is  $\sim 800$  ps). The top device exhibits a slow decay component that is not visible on the bottom one (the small oscillations just after the pulses are caused by signal bounces in non-perfectly adapted cables). Insets show the shapes of the detection signals observed under pulsed X-ray excitations at 20 keV and at 0.3 GHz.

in the top figure is much slower. The difference in materials results from the growth process: the ‘fast’ material is obtained using a low incorporation of nitrogen in the gas phase during growth (10–20 ppm) that is assumed to create a recombination centre, therefore reducing the carrier lifetime in the material. This also shows that the specific properties of the material can be adapted to the requirements of the measurement. In the top curve of Fig. 2, the signal decay can be closely fitted by a double exponential with a slow decay characteristic at 17 ns that has a much greater contribution to the overall signal. The fast device has been successfully used for the temporal characterization of the bunch distribution of the synchrotron light structure (352 MHz) at the ESRF (Fig. 3; Bergonzo, Brambilla *et al.*, 2000). However, the same measurement performed on the slow device would have been severely affected by a rising baseline level, resulting from the slow decay time, superimposed on the signal. This is illustrated in the insets of Fig. 2. It further demonstrates that small changes in the growth conditions can result in films with extremely differing characteristics for their use as radiation detectors.

## 5. Influence of the polycrystalline structure on the non-uniformity of the sensitivity

Since we are focusing here on the case of thin polycrystalline layers, with grain sizes typically of the order of 10 to 20% of the thickness, one inherent drawback with CVD diamond is that regions of degraded properties are likely to be observed within the grain boundaries, which may result in non-uniformity of the detector response.

Experiments were also performed at the ESRF using a microfocused X-ray beam to image sensitivity maps of detector-grade polycrystalline diamonds. The experiments were performed using the scanning X-ray microscope of the ID21 X-ray microscopy beamline (Barrett *et al.*, 1998) which provided a focused X-ray microprobe. The beam was here monochromated to provide an incident photon energy of

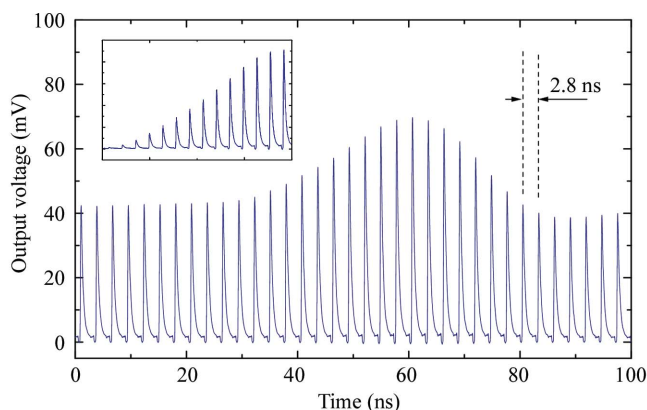


**Figure 3** Evidence of non-uniformity of the bunch train of the two-thirds filling mode at ESRF. The inset shows the linear rise of the individual X-ray pulse intensity at the beginning of the bunch train. Measurements were confirmed by machine diagnostics. This device enables the direct monitoring of the X-ray beam intensity and temporal distribution of the white beam, mostly 8–20 keV.

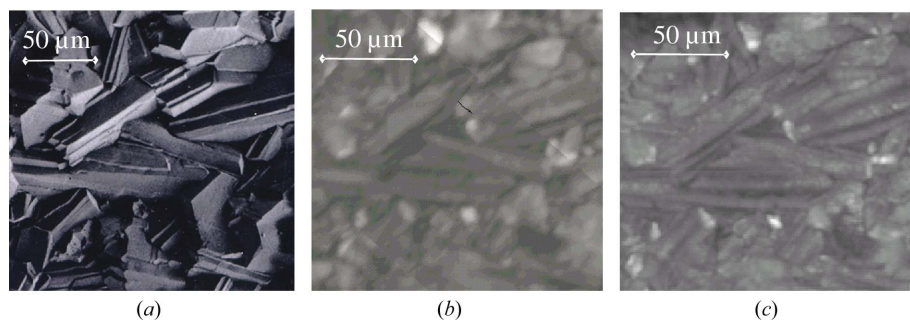


**Figure 4** (a) SEM image of the region of interest. The sample is 150  $\mu\text{m}$  thick. (b) Map of the X-ray response observed in the region displayed in (a) using a micrometer-size focused X-ray beam at 6 keV. The sensitivity of the detector appears to be closely dependent on the material as the grain structure can be clearly recognized. (c) Same map but measured at 3 keV (see text).

correlation between the polycrystalline structure and the response of the detector.

The same measurement was also conducted at 3 keV, an energy at which the attenuation length in diamond is 30  $\mu\text{m}$ . Here the charge generation is assumed to occur mostly in the vicinity of the surface layer. The scan was performed using a lower flux of  $1.2 \times 10^8$  photons  $\text{s}^{-1}$  into the same spot size. The map probed on the same region as Fig. 4(a) is plotted in Fig. 4(c). It shows that the scan at lower energy also strongly resembles that of Fig. 4(b) obtained at 6 keV, and the SEM image.

One conclusion is that most of the signal observed is due to the front layer, *i.e.* the region where the grains are bigger owing to the columnar growth of diamond.

From the preceding statement that most of the signal actually appears to be created in the vicinity of the surface of the non-polished CVD sample, *i.e.* where the grains are bigger, one approach to improve the device sensitivity is to use big-grain materials, fabricated from the growth of very thick layers, which are thinned using abrasion and/or lapping to a significant depth from the substrate side. This approach has been commonly used for the fabrication of high charge transport property material as initially developed for high-energy physics detection and that is now provided on a commercial basis by Element Six. If a similar measurement to that described in the preceding section is performed on this bigger-grain material, evidence of stronger discrepancies in the material sensitivity can be observed, as shown in Fig. 5(a). The map of the sensitivity is probed here at 5.5 keV in a 1 mm  $\times$  1 mm region located in one corner of the square gold contact. Unfortunately the polished nature of this diamond layer does not allow the comparison with the grain structure as could be observed using SEM. In the sensitivity map of this probed area, islands are clearly visible that could be attributed to the grain structure of the material of the order of 80  $\mu\text{m}$  in size. By zooming into the region marked by a rectangle in Fig. 5(a), and using a step displacement of 1  $\mu\text{m}$  for the scan, a sensitivity map of greater resolution was probed and is shown in Fig. 5(b). The grain boundaries are now observed and they appear as black lines displaying lower sensitivities. At this incident energy (5.5 keV), the figure shows a through thickness average of the diamond layer which highlights the presence of grain boundaries, dislocations or simply regions of lower sensitivities. The sensitivity varies from 20 to 60% as a function of the beam-position interaction on the diamond device.

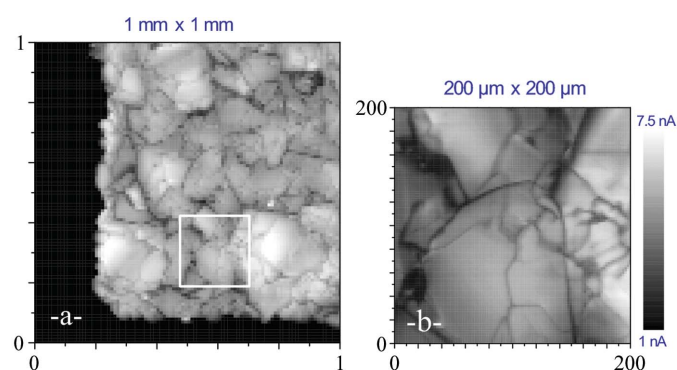


**Figure 5** (a) Image of the X-ray sensitivity as measured on a 1 mm  $\times$  1 mm area in the corner of the electrical contacts. The grey scale is logarithmic and given in nA for a  $2.2 \times 10^8$  photons  $\text{s}^{-1}$  flux at 5.5 keV. (b) Zoom on the 200  $\mu\text{m}$   $\times$  200  $\mu\text{m}$  region indicated.

6 keV using a double-crystal fixed-exit monochromator (Si 111) with an X-ray beam flux of approximately  $10^{10}$  photons  $\text{s}^{-1}$  into a spot size of diameter 1  $\mu\text{m}$ . The diamond sample was placed perpendicular to the beam axis in the focal plane of a Fresnel zone plate lens, with the X-rays impinging on the diamond through a 100  $\text{\AA}$  gold layer electrical contact. At 6 keV, the attenuation of the incident X-rays induced by this gold layer is below 1%. Measurements were also made in the region shown in the scanning electron microscopy (SEM) image shown in Fig. 4(a). The picture is taken through the 100  $\text{\AA}$  gold layer, and reveals that the Au coating is uniformly covering the diamond rough surface (no local polarization owing to surface charging artefacts). The device is 150  $\mu\text{m}$  in thickness and does not display any preferred orientation of the diamond crystallite grain morphology. The X-ray  $1/e$  attenuation length of diamond at 6 keV is approximately 250  $\mu\text{m}$ , therefore the excitation can be considered as taking place through the entire thickness. Fig. 4(b) displays a map of photosensitivity recorded as the focused X-ray beam is scanned across the region shown in Fig. 4(a). Strong variations in the sample sensitivity are observed along its surface. Comparison of the SEM image and the map of the X-ray photo-induced currents reveal a strong

## 6. Polycrystalline beam-position monitors and performance

Fig. 6 shows the structure of a four-quadrant beam-position monitor (BPM) device. The polycrystalline diamond layer was

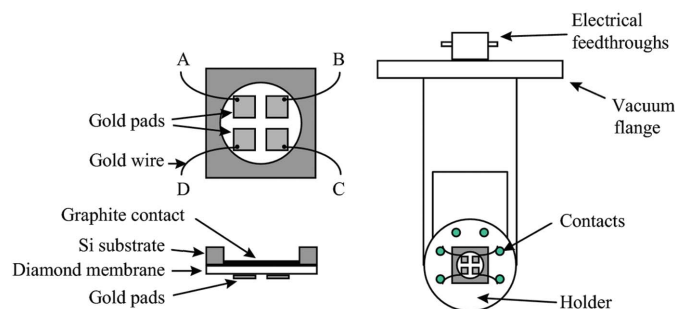


**Figure 6** Schematic view of the diamond BPM (left), and complete device (right). The device can be mounted on a standard vacuum manipulator.

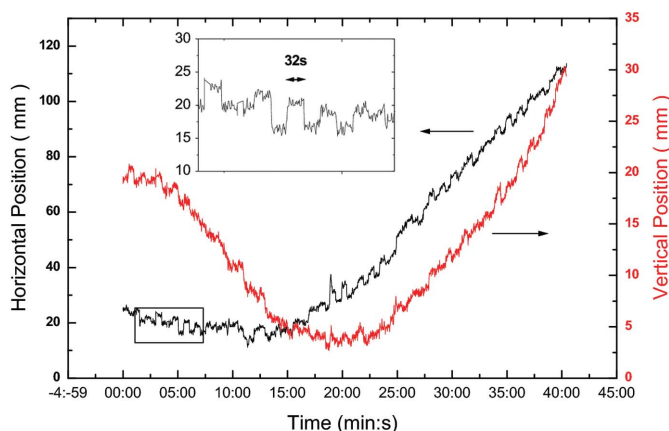


**Figure 7** Time-scan measurements using the diamond BPM detector, revealing typical beam-position shifts. The beam energy is 4 keV and the beam size is  $200\ \mu\text{m} \times 200\ \mu\text{m}$ . The inset shows a small ( $\sim 2\ \mu\text{m}$ ) periodical displacement as induced by the machine global feedback.

grown on a silicon substrate by the CVD technique, making it possible to back etch a hole in the silicon to obtain a thin diamond membrane supported by a silicon ring. This technique enables diamond layers as thin as  $10\ \mu\text{m}$  to be used as BPMs, therefore enabling the semi-transparent monitoring of extremely short wavelengths. On one side of the diamond an ultra-thin electrical contact is used that provides a low cross section to X-rays. In fact, graphite is the best material as it does not add any other atomic number material in the beamline that could be detrimental for precision absorption spectroscopy experiments. The front graphite electrodes are obtained by electron beam evaporation. On the other side the contact is divided into four sections, leaving a central region with no contact material. This is important as the high position sensitivity of this type of device here relies on the field decay at the central edge of these contacts pads. By accurate measurement of the photocurrents in each of the four contacts, *e.g. via* the use of an electrometer, it is easy to measure the beam centroid. In fact, when the photon flux interacts in the diamond, it generates free carriers (electrons and holes) that will drift along the electric field and induce a current in the four electrodes. When the four currents are

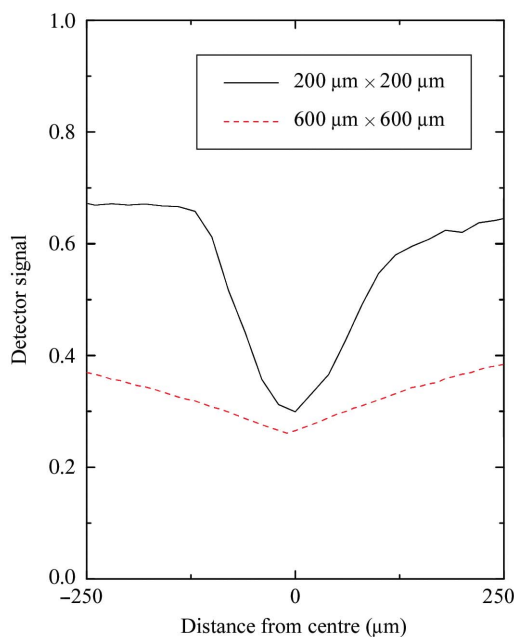


**Figure 8** Evolution of the electrode currents in the centre of the BPM device, as a function of the beam size.

equal, the gravity centre of the X-ray beam can be located with high resolution. A typical time-scan measurement is shown in Fig. 7, obtained at 4 keV with a  $200\ \mu\text{m} \times 200\ \mu\text{m}$  beam size and on a BPM with  $500\ \mu\text{m}$  electrode gap spacing. It reveals the drift of the horizontal and vertical positions of the X-ray beam, with almost a  $40\ \mu\text{m}$  shift over 20 min. A closer observation (see inset) reveals smaller periodical shifts which correspond to the global feedback period of 32 s of the electron beam position in the storage ring. Such instabilities can be detrimental to experiments where the position is crucial. Displacements smaller than  $2\ \mu\text{m}$  could be clearly observed, and illustrate the excellent performance of the diamond BPM. The semi-transparent diamond-based BPM provides information on the online correction of these shifts even at low X-ray energies.

One inherent drawback, however, of this specific four-quadrant configuration, *i.e.* where the positioning contacts are at the periphery of the beam, is that the BPM resolution depends on the size of the beam, as is visible in Fig. 8 (where the width of the abscissa scale here corresponds to the gap spacing of  $500\ \mu\text{m}$ ). Another configuration was therefore developed, based on the use of a resistive layer, with a  $0.1\ \mu\text{m}$ -thick layer of boron-doped amorphous silicon (a-Si:H) with a resistivity of  $10^5\ \Omega\ \text{cm}$  (Fig. 9). Here, the current induced in the diamond is detected in each of the four corners of the a-Si:H layer, which are connected to the four channels of the electrometer. The induced current in each pad varies linearly with the distance between the beam interaction position and the pads (Fig. 10). Other configurations can also be of interest and, for example, beam monitors consisting of a set of several strip electrodes have been developed that enable profile monitoring with a  $20\ \mu\text{m}$  pitch resolution (Bergonzo, Tromson *et al.*, 2000).

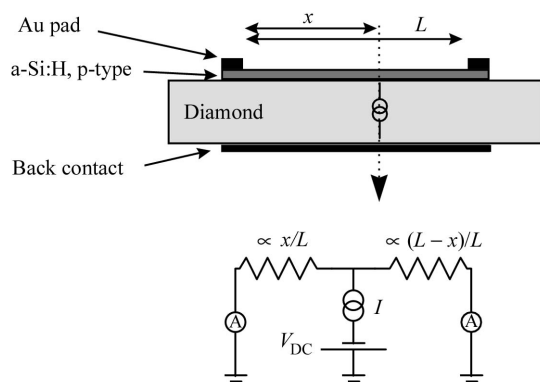


**Figure 9**  
Schematic representation of the resistive readout beam-position monitor.

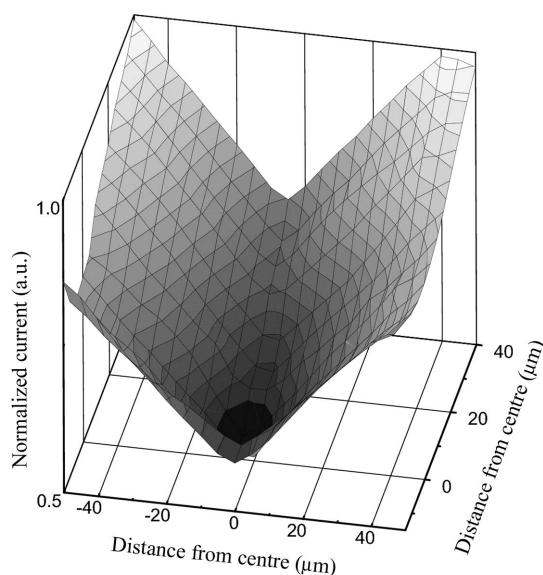


**Figure 10**  
Maximum individual currents in the resistive readout device on a 50  $\mu\text{m}$  scale. Each current varies linearly as a function of the interaction position from the centre of the device. The figure has been reduced to half of the device for clarity (energy here is 6.2 keV, beam size 200  $\mu\text{m}$   $\times$  200  $\mu\text{m}$ ).

## 7. Conclusions

The potential of diamond films grown in our laboratory using the CVD technique for the characterization of X-ray light sources as encountered in synchrotrons has been described. Specific inherent properties such as the high radiation and temperature hardness of diamond enable the fabrication of detection devices that exploit its low atomic number for reduced X-ray cross section, and also its short carrier lifetime for ultra-fast pulse monitoring. Here we have demonstrated that polycrystalline materials show high potential for this type of measurement. From the design of thin ionization chambers it is feasible to fabricate beam-position monitors, and other structures are readily achievable that could enable the fabrication of profile monitors for example (Bergonzo, Tromson *et al.*, 2000). These CVD diamond detectors demonstrate the unique feature of enabling position and profile measurements of low-energy synchrotron X-ray light sources, together with a low attenuation of X-ray photons, thus allowing real-time

monitoring of the beam with excellent position sensitivity. The signal measurements could be made for example using four-channel electrometers that are commercially available. Furthermore, very simple low-cost and radiation-hard devices can be fabricated in order to enable the measurement of the temporal distribution of the X-ray beam intensity distribution, with ultra-fast time responses well below 1 ns.

Many of the results presented here have been obtained from beamline time and facilities provided by the ESRF. The authors would like to acknowledge the ESRF for having granted beam time to the following application for experiments: MI212 (ID26 + ID12); MI258 (ID26), MI347 (ID21), MI380 (ID26), MI452, MI541, MI609, MI679 (all ID21). The work on diamond BPMs was initiated by C. Gauthier in 1997. J. Goulon and A. Sole are also acknowledged for their contributions. We thank S. Feite from the ID-26 support team for technical help. All the microbeam photocurrent studies were performed with R. Barrett who is gratefully acknowledged together with J. Susini and the ID21 beamline team. The authors are also greatly indebted to other partners such as A. Thompson (now at Soleil); J. Morse and W. Shepard for the work at ID29 and useful discussions. The study on temporal response monitoring was conducted in close collaboration with R. Wrobel's team from CEA/DAM in Bruyères le Chatel, and partners from ESRF, namely J.-F. Eloy and O. Mathon.

## References

- Alkire, R. W., Rosenbaum, G. & Evans, G. (2000). *J. Synchrotron Rad.* **7**, 61–68.
- Aoyagi, H., Kudo, T. & Kitamura, H. (2001). *Nucl. Instrum. Methods Phys. Res. A*, **467–468**, 252–255.
- Ascarelli, P., Cappelli, E., Pinzari, F., Rossi, M.-C., Salvatori, S., Merli, P.-G. & Migliori, A. (2001). *J. Appl. Phys.* **89**, 689–696.
- Barrett, R., Bergonzo, P., Snidero, E. & Delacour, P. (2002). ESRF Experiment Report MI 541. ESRF, Grenoble, France.
- Barrett, R., Kaulich, B., Oestreich, S. & Susini, J. (1998). *Proc. SPIE*, **3449**, 80–90.
- Behnken, T., Oh, A., Wagner, A., Zeuner, W., Bluhm, A., Klages, C.-P., Paul, M. & Schafer, L. (1998). *Diamond Relat. Mater.* **7**, 1553.
- Bergonzo, P., Brambilla, A., Tromson, D., Mer, C., Guizard, B. & Foulon, F. (2000). *Appl. Surf. Sci.* **155**, 179–185.
- Bergonzo, P., Foulon, F., Brambilla, A., Tromson, D., Jany, C. & Haan, S. (2000). *Diamond Relat. Mater.* **9**, 1003–1007.
- Bergonzo, P., Tromson, D., Brambilla, A., Mer, C., Guizard, B. & Foulon, F. (2000). *Applications of Synchrotron Radiation Techniques to Materials Science, Materials Research Society Symposium Proceedings Series*, Vol. 590, p. 125. Warrendal, PA: Materials Research Society.
- Foulon, F., Bergonzo, P., Borel, C., Marshall, R. D., Jany, C., Besombes, L., Brambilla, A., Riedel, D., Museur, L., Castex, M. C. & Giquel, A. (1998). *J. Appl. Phys.* **84**, 5331–5336.
- Franklin, M., Fry, A., Gan, K. K., Han, S., Kagan, H., Kanda, S., Kania, D., Kass, R., Kim, S. K., Malchow, R. *et al.* (1992) *Nucl. Instrum. Methods Phys. Res. A*, **315**, 39–42.
- Guerrero, M.-J., Tromson, D., Rebisz, M., Mer, C., Bazin, B. & Bergonzo, P. (2004). *Diamond Relat. Mater.* **13**, 2046.

- Holldack, K., Ponwitz, D. & Peatman, W. B. (2001). *Nucl. Instrum. Methods Phys. Res. A*, **467–468**, 213.
- Isberg, J., Hammersberg, J., Johansson, E., Wikstrom, T., Twitchen, D. J., Whitehead, A. J., Coe, S. E. & Scarsbrook, G. A. (2002). *Science*, **297**, 1670–1672.
- Kozlov, S. F., Belcarz, E., Hage-Ali, M., Stuck, R. & Siffert, P. (1974). *Nucl. Instrum. Methods*, **117**, 277–283.
- Kozlov, S. F., Stuck, R., Hage-Ali, M. & Siffert, P. (1975). *IEEE Trans. Nucl. Sci.* NS-22, 160.
- Kuzay, T. M. & Shu, D. (1995). US Patent 5387795.
- Loudin, L., Mikhailov, V., Rezvov, V., Artemev, A., Peredkov, S., Rakhimbabev, T., Lemonnier, M., Megtert, S. & Rouillay, M. (1998). *Nucl. Instrum. Methods Phys. Res. A*, **405**, 265–268.
- Mer, C., Pomorski, M., Bergonzo, P., Tromson, D., Rebisz, M., Domenech, T., Vuillemin, J. C., Foulon, F., Nesladek, M., Williams, O. A. & Jackman, R. B. (2004). *Diamond Relat. Mater.* **13**, 791–795.
- Morse, J., Whitehead, A. J., Twitchen, D. J. (2006). In preparation.
- Nam, T. L., Rijn, J. V., Keddy, R. J., Fallond, P. J. & Schlimmer, J. F. (1992). US Patent 5128546.
- Ristein, J., Riedel, M., Maier, F., Mantel, B. F., Stammer, M. & Ley, L. (2001). *J. Phys. Condens. Matter*, **13**, 8979–8987.
- Sakae, H., Aoyagi, H., Oura, M., Kimura, H., Ohata, T., Shiwaku, H., Yamamoto, S., Sugiyama, H., Tanabe, K., Kobashi, K. & Kitamura, H. (1997). *J. Synchrotron Rad.* **4**, 204–209.
- Scarsbrook, G. A., Martineau, P. A., Dorn, B. S. C., Cooper, A. M., Collins, J. L., Whitehead, A. J. & Twitchen, D. J. (2001). Int. Patent Appl. WO 01/96634 A1.
- Schulze-Briese, C., Ketterer, B., Pradervand, C., Bronnimann, Ch., David, C., Horisberger, R., Puig-Molina, A. & Graafsma, H. (2001). *Nucl. Instrum. Methods Phys. Res. A*, **467–468**, 230–234.
- Shu, D. (1999). *17th Advanced Beam Dynamics Workshop on Future Light Sources*, 6–9 April 1999, Argonne National Laboratory, IL, USA.
- Shu, D. & Kuzay, T. M. (1995). US Patent 6037596.
- Silfhout, R. G. van (1999). *J. Synchrotron Rad.* **6**, 1071–1075.
- Souw, E. K. & Meilunas, R. J. (1997). *Nucl. Instrum. Methods Phys. Res. A*, **400**, 69–86.
- Tromson, D., Bergonzo, P., Brambilla, A. & Foulon, F. (2000). *J. Appl. Phys.* **87**, 3360.